A 2D Random Walk Mobility Model for Location Management Studies in Wireless Networks

Kuo Hsing Chiang, RMIT University, Melbourne, Australia
Nirmala Shenoy, Information Technology Department, RIT, Rochester, NY 14623. USA, ns@it.rit.edu

Abstract:
In this work a novel 2D random walk mobility model is proposed that can be used for studying and analysing location area crossing rate and dwell time of mobile users in wireless networks. The development and application of the model under two cell structures, namely the square cell and the hexagonal cell have been detailed. The analytical results obtained for location update rates and dwell times have been validated using simulated and published results. The highlights of the model are its simplicity, minimal assumptions, and adaptability to conduct both 'location crossing rate' and 'dwell time' studies using the same model with slight modifications for the square cell or the hexagonal cell. Using symmetry of mobile-user movement, reduced number of computational states was achieved. A novel wrap-around feature of the model, facilitates reduced assumptions on the user mobility and has reduced the mathematical computation complexity considerably. A regular Markov chain model was used for computing average location area crossing rate. A slightly modified model with absorbing states was used to derive the dwell time. This is the first model of its kind that can be used for studying area-crossing rates. To further emphasize the flexibility of the model we have extended the model to study an overlapped location area strategy. The study and analysis of overlapped locations areas has hitherto been difficult, due to the complexity of the models.

I. Introduction

Mobility of users is a major advantage of wireless over fixed telecommunications systems. The signaling traffic and database processing to support mobility of users are always the key concerns in the design and performance of wireless networks. Mobility models play a key role in studying different mobility management features such as registration, paging, handoff, and database approaches. A mobility model with minimum assumptions and which is simple to analyze will be very useful under such circumstances. In most wireless network performance studies the cell is assumed to be either hexagonal or square in shape [1], though in real life cell shapes may be highly irregular. Some authors assume a circular cell shape, especially those using a fluid flow model. However in our work we have restricted our analysis to hexagonal and square cells, and the model we propose can easily accommodate these two types of cell shapes.

In this work we highlight a novel 2D random walk model that it can be used for studying and analyzing location area crossing rate and dwell time of mobile with slight modifications to the basic proposed model. The development and application of the model under two cell structures, namely the square cell and the hexagonal cell have been detailed. In both cases the analytical results obtained for location update rates and dwell times have been validated using simulated and published results. The analytically obtained results from the model show excellent concurrence (relative error of less than 1%) with the simulated and published results. The highlights of the model are its simplicity, minimal assumptions, and adaptability to conduct both location crossing rate and dwell time studies using the same model with slight modifications for both square and hexagonal cells. We have used mobile-movement symmetry within and across 'location areas' and applied the 'lumped process' property of Markov chains to obtain a model with reduced computational states. A novel wrap-around feature has been used in these models to reduce constraints on mobile movements, thereby providing a more realistic roaming scenario. The model uses a set of aggregate states to trace user movement within one location area and then uses a set of special (asterisk) states when crossing the boundary of the location area. Due to the wrap-around technique, the movement of the mobile is modeled to again enter the original states from the special states, once the mobile starts moving within the new location area. Average number of location area crossing rates or updates made by the user is obtained by solving for the regular Markov chain. A slightly modified model with absorbing states was used to derive the dwell time. This is the first model of its kind that can be used for studying area-crossing rates and dwell times using a simple model. To further emphasize the flexibility of the model we extended the model to study an overlapped location area strategy. We have provided comparative results between the overlapped and the non-overlapped strategies. Overlap location area strategies are commonly used concepts in cellular networks. However the study and analysis of such overlapped configurations has been difficult, due to the requirement of complex models. We show that by using the proposed model it is possible to study such overlapped location area schemes.

Numerous works can be found in the literature that address mobility modeling and various models have been proposed by researchers to efficiently apply analytical and simulation models for mobility studies. Below we highlight some of these models. At the end of this section, we highlight those features of our model, which makes it simple to use and adaptable to various mobility studies.

The fluid flow model [2, 3, 4, 14] and random walk model are the two main types of mobility model that have been applied in location management studies. The fluid flow model can derive the average rate of boundary crossings per unit time out of a given area, but it is difficult to apply the model to the modern per-user based location area strategies or to study overlapped area strategy performance. Most random walk models are designed for dynamic location area strategy [6, 7] or for deriving the dwell time [1, 5]. In [1], the authors have proposed a random walk model, but requires solving for complex mathematical equations, which we were able to avoid due to the wrap-around mechanism. In [11], Tuna et al propose a novel approach to mobility modeling capturing the moving-in groups, conscious traveling and inertial behavior of the subscribers in real life, using the locus of the mobile user in a terrain. In [12], a free space propagation model using GPS is proposed by the authors, which more suited to ad hoc networks. In [13] a three level model is proposed covering a city area model, area zone model and a street unit model.

Location areas can be dynamic or static. The proposed model can be adapted to study location area crossing rates and dwell time in both dynamic as well as static location area strategies. The simple 2-D random walk model is based on the properties of the regular and absorbing Markov chain. The regular model is used for computing the location update rates. The same model with absorbing states is used to derive the dwell time in an area. The number of computational states in the model is very less, making it s analysis is easy. A 'states wrap-around' feature has been introduced in the model, which facilitates estimating location update rate using simple equations. The model can be adapted to both square cell and hexagonal cell structures. Because of the simplicity in calculations, the model can be extended to study overlapped location areas strategies, which has hitherto been difficult to handle. These are features, which make the model ideally suited to mobility management studies in cellular networks, though with limitation that the cells will be either square or hexagonal.

Section II describes the development of the two-dimensional random walk mobility model for both square and hexagonal cell clusters. In section III, the mathematical analysis for location update and dwell time for both cell structures are described. Section IV provides model validation by providing comparative results from the analytical model, a simulated model and published results. Highlights of the model are given in section V and conclusion in section VI.

II. The 2D Random Walk Model

Users in cells belonging to a Location Area (LA) have identical movement pattern within and across LAs. Such cells can be assigned to a single state in the Markov chain using the lumped process property. This property has been applied here to achieve reduced computational states in the model. A state which lumps a number of cells with identical movement pattern is called an 'aggregate state'. In the following two subsections the derivation of the 2D random walk model for the square cell and hexagonal cell are presented.

A. Model for Square Cells

Fig. 1A shows an LA configuration for n*n square cells where n = 5. The bold lines indicate the boundary of the LA. Cells in the adjacent LAs are shown outside the thick boundary lines. There are 25 cells in the LA and they have been numbered, identifying each cell with its row and column position. It is assumed that the mobile user can make movement in 4 directions only with an equal probability of ¼ in each direction as shown in Fig. 1B. In Fig 1A arrows show the possible user movement across cells within one LA and across LAs. In some of the cells, with reference to the LA, the mobile user will have identical movement patterns to other cells within the same LA and to cells in adjacent LAs. For e.g. from cells numbered 11, 15, 55 and 51 the mobile user movement pattern and transition probabilities will be identical but rotated by 90 degrees. The rotation of the movement pattern will not affect the studies to be conducted using Markov chains. Hence these four cells can be grouped into one aggregate state in the Markov chain model. This property of lumping the states was carried out to reduce the total number of computational states in the mathematical analysis. An algorithm to perform state aggregation is given below (Figs 2A and 2B are provided for the purpose of explaining the aggregation process)

1. Number the cells belonging to an LA as 'rc' where r is the row number and c is the column number as shown in Fig 1A. The numbering scheme has been applied to the cells in the adjacent LAs also i.e. cells just outside the bold lines.
2. As shown as in Fig. 2A assign the cells to different loops. In this case there are 3 loops. Let l = number of loops. Then l=1 is the outer loop, l=2 is the next loop and l=3 is the innermost loop. Cell 33 belongs to loop 3. Cells numbered 22, 23, 24, 34, 44, 43, 42, 32 belong to loop 2. The rest of the cells in the LA belong to loop 1.
3. Start with n =5, l=1

   Until (n =l)

   Repeat { x= l; y = n;

   Until(x > y)

   Repeat { set S_l^x = {Src ∪ Scr}

   Where r = l for c = x, y and r = n for c = x, y

x = x +1; y = y-1;
}
n = n-1, *l*= *l*+1;
}

S_l^x - is the aggregate state obtained as a set of the cells Src and Scr where, Src is the cell numbered 'rc' and Scr is the cell numbered 'cr'

After the aggregation process the following state aggregation is obtained

$S^1_1 = \{S_{11}, S_{51}, S_{15}, S_{55}\}$,
$S^1_2 = \{S_{21}, S_{25}, S_{41}, S_{45}, S_{12}, S_{52}, S_{14}, S_{54}\}$,
$S^1_3 = \{S_{31}, S_{35}, S_{13}, S_{53}\}$.
$S^2_1 = \{S_{22}, S_{24}, S_{42}, S_{44}\}$,
$S^2_2 = \{S_{32}, S_{34}, S_{23}, S_{43},\}$.
$S^3_1 = \{S_{33}\}$.

For ease-of-use, the aggregate states were assigned numbers as shown below.

$S^1_1 \rightarrow 1$, $S^1_2 \rightarrow 2$, $S^1_2 \rightarrow 3$, $S^2_1 \rightarrow 4$, $S^2_2 \rightarrow 5$, $S^3_1 \rightarrow 6$.

We now have 6 aggregate states. The LA is redrawn in Fig. 2B with the cells numbered with their newly assigned aggregate state numbers. In Fig. 2B aggregate states 1, 2 and 3 are in the boundary of the LA and are called the 'boundary' states. We further define 'asterisk boundary' states (or 'star states') i.e. 1^*, 2^* and 3^*, which are the boundary states in the adjacent LAs. Let LA0 be the LA under consideration then in Fig 2B, LA1, LA2, LA3 and LA4 are the adjacent LAs. From LA0 a user can move only into any one of these adjacent LAs.

Using the direction and movement probabilities given in Fig. 1B, the state transition diagram for the regular Markov chain based on the aggregate states can be derived as shown in Fig 3. In this approach the entire movement of the mobile user across different cells and across LAs is modeled. The 'asterisk boundary' states and the wrap around mechanisms, which will be explained shortly, achieve this freedom-of-movement feature. Movement into an 'asterisk' boundary state indicates a location area crossing and can be used to study the location area crossing rates or location updates.

A brief description of the operation of the state transition diagram of Fig. 3 is now provided. As long as the user moves within cells in a location area, he is in one of the main aggregate states i.e. 1, 2, 3, 4, 5 or 6. His movement is accordingly traced by the transitions shown. Transition probabilities are marked beside the transition. The dotted transitions to the asterisk states indicate the mobile user's transition to a boundary state in an adjacent location area and the probabilities of such transitions are given besides these dotted transitions. These transitions accordingly model the mobile user's movement probability from the main location area cells to the adjacent location area cells. While in an asterisk states the user can move across to other asterisk states. For e.g. (in Fig 2B) the user move from 1* in LA3 to 1* in LA7 or from 2* in the adjacent LA3 back to 2 in LA0 (2 in LA0 now would be 2* from the mobile user perspective as it is in an adjacent LA). In Fig. 3, this movement is modeled by the dotted transitions to itself in the asterisk states. Again, looking at the user movement from state 1* in LA3 (Fig 2B), the user has a probability of ¼ to move into state 1* in LA7, and probability of a ¼ to move into state 1 in LA0 (which is now state 1* in the adjacent LA from the user perspective) – hence a transition probability of ½ to itself in state 1* is shown in the Fig. 3.

When the user starts moving in the new LA, for e.g. when he moves from state 1* in LA3 to 2* in LA3 or from 2* to 1* in LA3 the model wraps back to the normal states – indicating that the user has now started moving in cells belonging to the new LA. This is shown by the dotted transitions from the asterisk states to the normal states in Fig 3. This novel wrap-around feature has subsequently led to the possibility of studying the location area crossings using simple equations.

This model can be applied at various levels of the network hierarchy. It can used to study the LA crossing and dwell time within one VLR (Visitor Location Area) and the traffic due to VLR crossing at the next higher level in the hierarchy. Examples provided below illustrate the use of this model only for location area crossing and area dwell time.

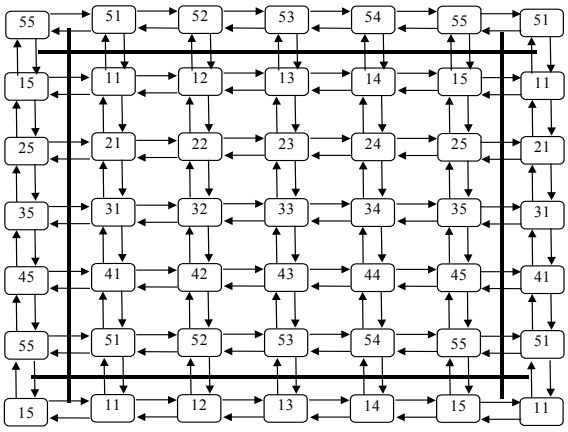

Fig. 1A

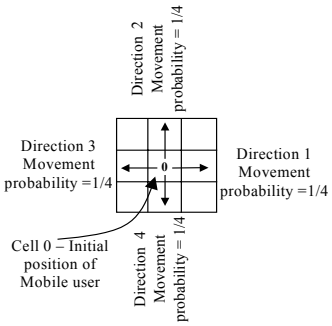

Fig. 1B

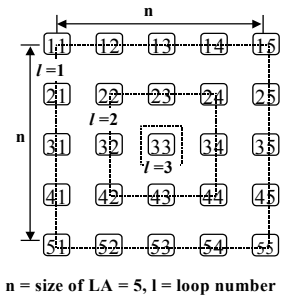

Fig. 2A

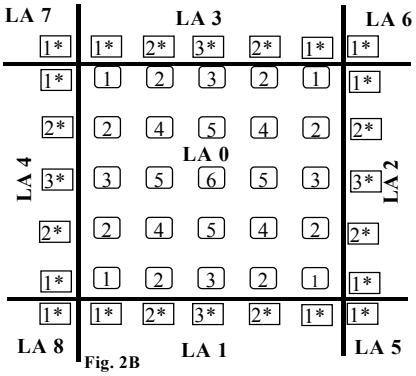

Fig. 2B

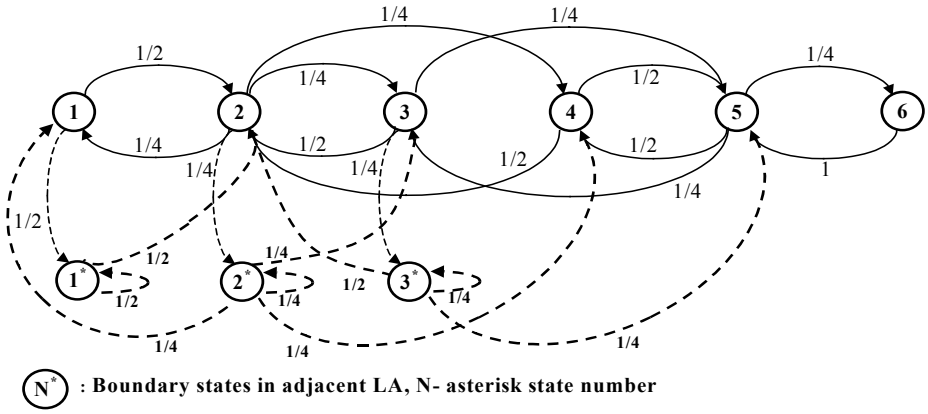

Fig. 3 State transition diagram for 5 * 5 square cell model

B. Model for Hexagonal Cells

The model is now applied to hexagonal cells. The cell or state aggregation process is slightly different and will be explained. Fig. 4A shows an LA of size n=4with hexagonal cells. Each LA covers '1+ $\sum_{l}^{n} n * 6$' i.e 61 cells if n = 4. As seen in Fig. 4B. the user movement is restricted to six direction with an equal probability of 1/6 in each direction. Following are the steps used for state aggregation.

1. The cells in the LA are assigned to loops and are numbered according to the loop they belong to. With reference to Fig. 4A all cells belonging to loop 1 are numbered 1, those belonging to loop 2 are numbered 2 and so on. Let *l* = number of loops. As can be seen there are 5 loops where loop 5 has only one cell.

2. Let l =1. Let c_{max} be the starting cell number. Set c_{max} = 1.
3. Starting from one corner of the hexagon move in a clockwise direction and allocate cell numbers starting from c_{max} = 1 in increasing order till the next corner is reached. Stop numbering at the cell just before the next corner cell.
4. Repeat step 3 starting from the next corner cell, till the outer loop is completed. The new cell numbers are shown in the unshaded cells in Fig. 4c. The maximum cell number allocated is 4 in loop l=1.
5. Set c_{max} = maximum cell number + 1.
6. In loop l = 2, start at the corner cell and move clockwise and start numbering from c_{max} in increasing order till the next corner is reached. As before stop at the cell just before the next corner.
7. Repeat from all corners in that loop, starting with the same c_{max} value, till all cells in the loop are numbered
8. Repeat step 5, 6 and 7 for the rest of the loops.

State aggregation has thus been completed. (The shaded cells in fig. 4C are the cells in the adjacent LA). From Fig. 4C, aggregate state 1 = {all cell marked 1}, 2 = {all cells marked 2}, and so on up. The states aggregation obtained is similar to [1] but uses a simple algorithm to perform the state aggregation.

As was done for the case of square cells, 'asterisk boundary' states are defined and identified in Fig. 4C for the hexagonal cells. There are 11 aggregate states and 4 asterisk boundary states in the Markov model. For the purpose of clarity the state transition diagram has been provided in 3 parts. Fig. 5A is the transition diagram for states or cells within a locations area. Figs 5B & 5C are for transitions across cells in the adjacent location areas. For the transition diagram, a similar explanation as used in the square cell case can be extended here and hence is not provided.

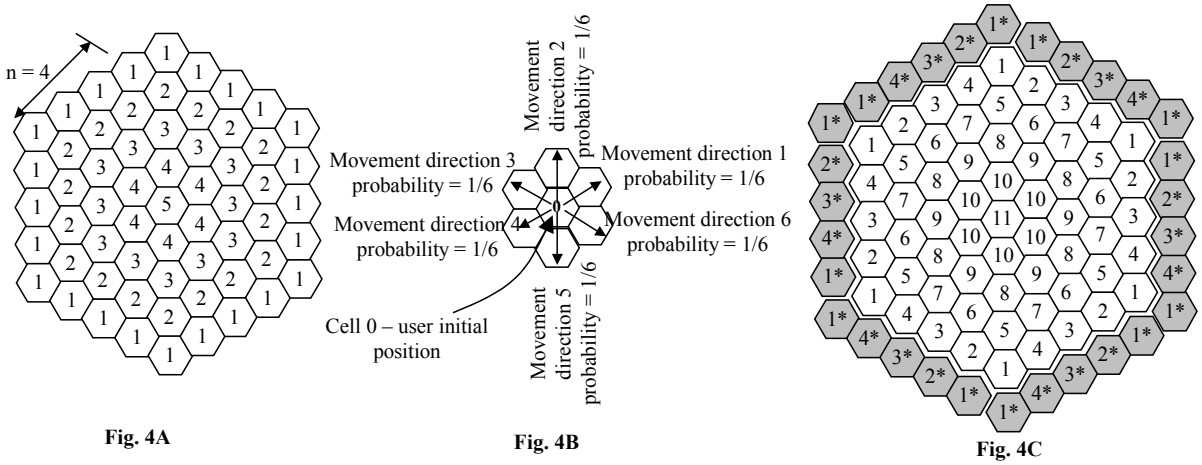

Fig. 4A **Fig. 4B** **Fig. 4C**

Fig. 4 Hexagonal cell LA

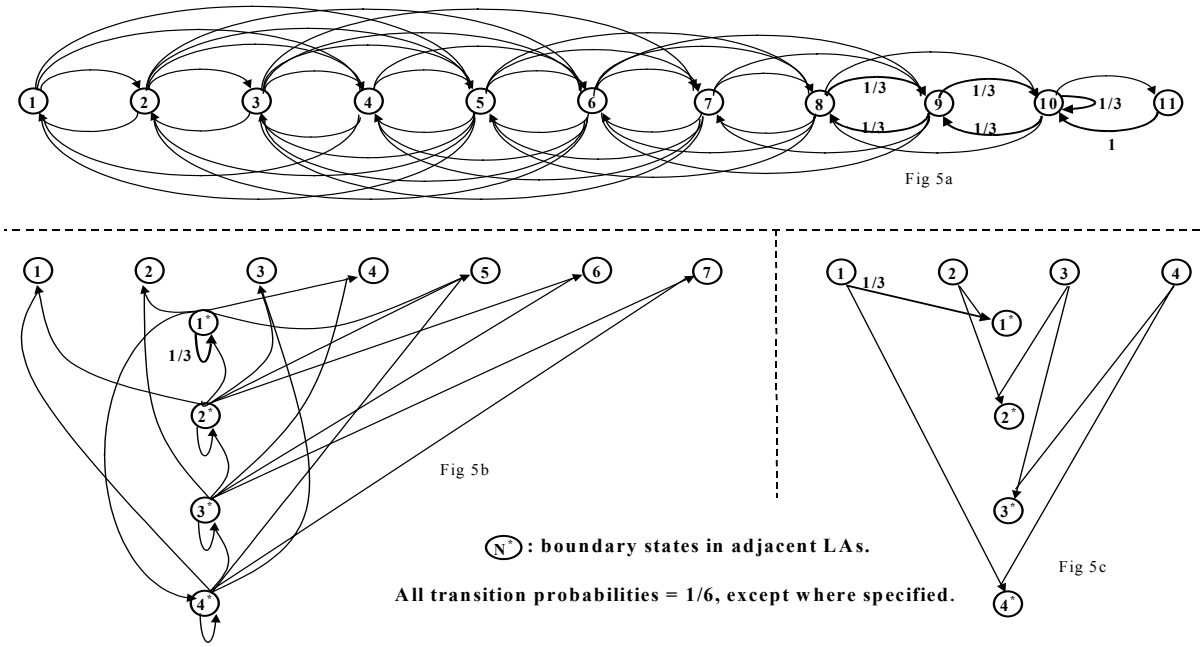

Fig. 5 State transition diagram for hexagonal cell model (n =4)

III. Model Analysis

It is assumed that each LA has similar properties and is of size n with n*n square cells or $1 + \sum_{1}^{n} 6n$ hexagonal cells. The state transition diagram for the Markov model for the user movement in LA comprising of square cells is shown in Fig.3. The state transition diagram for mobility in an LA comprising hexagonal cells is shown in Fig. 5. The general format for the transition probability matrix P in either case is given as

$$\mathbf{P} = [\, p_{ij} \,] = \begin{array}{c} \\ 1^* \\ 2^* \\ \vdots \\ N^* \\ 1 \\ 2 \\ 3 \\ \vdots \end{array} \begin{array}{c} \begin{array}{cccccccc} 1^* & 2^* & \cdots & N^* & 1 & 2 & 3 & \cdots \end{array} \\ \begin{pmatrix} p_{1^*1^*} & p_{1^*2^*} & \cdots & p_{1^*N^*} & p_{1^*1} & p_{1^*2} & p_{1^*3} & \cdots \\ p_{2^*1^*} & p_{2^*2^*} & \cdots & p_{2^*N^*} & p_{2^*1} & p_{2^*2} & p_{2^*3} & \cdots \\ & & \cdots & & & & & \\ p_{N^*1^*} & p_{N^*2^*} & \cdots & p_{N^*N^*} & p_{N^*1} & p_{N^*2} & p_{N^*3} & \cdots \\ p_{11^*} & p_{12^*} & \cdots & p_{1N^*} & p_{11} & p_{12} & p_{13} & \cdots \\ p_{21^*} & p_{22^*} & \cdots & p_{2N^*} & p_{21} & p_{22} & p_{23} & \cdots \\ p_{31^*} & p_{32^*} & \cdots & p_{3N^*} & p_{31} & p_{32} & p_{33} & \cdots \\ \cdots & & \cdots & & & & \cdots & \end{pmatrix} \end{array}$$

Where 1*, 2* …..N* are the asterisk boundary states for that configuration.

In the following subsections first a derivation of the LA update is provided and then the dwell time derivation is given. The subsection that follows briefly explains the simulation process.

A. Analysis for LA Updates

The state transition diagrams in Figs. 3 and 5 show that there no transient sets in the model but only a single ergodic set with only one cyclic class, hence the regular Markov chain properties can be applied to analyse the behaviour of the proposed model [10].

Let **P** be the regular transition probability matrix, then the steady state (limiting) probability vector $\boldsymbol{\pi}$ can be solved by the following equations:

$$\pi P = \pi \quad \text{and} \quad \sum_{i=1}^{m} \pi_i = 1, \tag{1}$$

where *m* is the number of states

P, the *fundamental matrix* for the regular Markov chain is given by :

$$\mathbf{Z} = [\, z_{ij} \,] = (\mathbf{I} - \mathbf{P} + \mathbf{A})^{-1} \tag{2}$$

where:
1. **A** is limiting matrix determined by **P**, and the powers $\mathbf{P}^n$ approach the probability matrix **A.**
2. Each row of **A** comprises of the same probability vector $\pi = \{\pi_1, \pi_2, \ldots, \pi_n\}$, i.e $\mathbf{A} = \xi\pi$, where ξ is column vector with all entries equal to 1
3. **I** is identity matrix.

The matrix **Z** can be used to study the behaviour of the regular Markov chain and using this matrix one can compute the mean number of times the process is in a particular state [10].

Let $y_j^{(k)}$ be the number of times that a process is in the state S_j in the first k steps, then if $M_i [y_j^{(k)}]$ is the mean number of times the process is in state S_j starting from state S_i is given by

$$M_i [y_j^{(k)}] \rightarrow (z_{ij} - \pi_j) + k\pi_j \tag{3}$$

The total number of boundary updates in k steps starting from state S_i can be computed by the total number of times that the process is in the asterisk states (for e.g. 1^*, 2^* and 3^* in Fig. 3) starting from state S_i – the initial state. Hence if U_{A_LA} is the average number of location updates in the analytical model, this is given by

$$U_{A\_LA} = M_i [y_{1*}^{(k)}] + M_i [y_{2*}^{(k)}] + M_i [y_{3*}^{(k)}] \tag{4}$$

Generalizing

$$U_{A\_LA} = \sum_{n=1^*}^{N^*} M_i [y_n^{(k)}] \tag{5}$$

Where 1*, 2* ….N* are the asterisk states in the model

B. Analysis for Dwell Time

To study the dwell time in a location area, the transition diagram of Fig. 3 and Fig. 5 are modified by converting the asterisk boundary states into an absorbing state. The transition diagram of Fig. 3 is reproduced as Fig. 6 to demonstrate the modification of the regular model into an absorbing Markov chain.

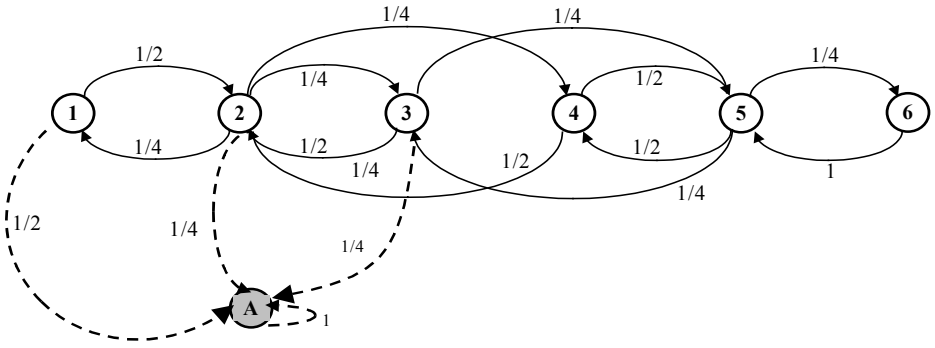

A :**Absorbing State** **Fig. 6 Absorbing Markov chain for the square cell model**

According to the property of an absorbing state, once it is entered, it cannot be left. Hence there is self-transition to this state with probability 1. By using the properties of the absorbing Markov chain, we can derive the LA dwell time (time to LA update), which is equal to the time to absorption. The transition matrix generally is given by

$$\mathbf{P} = \left[\begin{array}{c|c} \mathbf{I} & \mathbf{0} \\ \hline \mathbf{R} & \mathbf{Q} \end{array}\right], \tag{6}$$

I: absorbing states
R: one step transition probability from non-absorbing state to absorbing states
Q: one step transition probability from non-absorbing state to non-absorbing states

The fundamental matrix for an absorbing Markov chain is obtained as

$$\mathbf{N} = (\mathbf{I} - \mathbf{Q})^{-1} \tag{7}$$

Let **t** be the function for the number of steps in which the process is in a transient state. In an absorbing chain this is the time to absorption. From [5, 10], the mean time to absorption from initial state S_i is given by

$$M_i [\mathbf{t}] = N\xi = U_{A\_D}, \tag{8}$$

which is the row sums of fundamental matrix, N where ξ is the column vector with all entries 1. U_{A_D} is the average dwell time, for a user residing in initial state *Si*.

C. Simulation

Simulation of the user mobility was done using simple Monte Carlo methods. In each iteration of the simulation, a set of random numbers is generated. Those random numbers are distributed uniformly on [1, 2, 3, 4] for square cell model, and on [1, 2, 3, 4, 5, 6] for hexagonal cell model. Based on the random number the user moves to one of the adjacent cell from a starting cell 0.

Whenever the MT moves across the LA boundaries, the counter for location update is increased by 1. If the total number of iterations is M_E = 100,000, then the average number of location update is calculated by:

$$U_{S\_LU} = \frac{1}{M_E} \sum_{x=1}^{M_E} M_i(x) \tag{9}$$

where x is the x^{th} experiment and has the x^{th} random number set and sequence.

IV. Model Validation

A. Location Update Rate- Square Cell Model

The number of computational states required for the 5 × 5 square shaped model is 9 (6 normal aggregate states plus 3 asterisk states). The regular transition matrix for this model derived from Fig 3 is given below:

$$\mathbf{P} = [\, p_{ij} \,] = \begin{array}{c} \\ 1^* \\ 2^* \\ 3^* \\ 1 \\ 2 \\ 3 \\ 4 \\ 5 \\ 6 \end{array} \begin{array}{c} \begin{array}{ccccccccc} 1^* & 2^* & 3^* & 1 & 2 & 3 & 4 & 5 & 6 \end{array} \\ \begin{pmatrix} 1/2 & 0 & 0 & 0 & 1/2 & 0 & 0 & 0 & 0 \\ 0 & 1/4 & 0 & 1/4 & 0 & 1/4 & 1/4 & 0 & 0 \\ 0 & 0 & 1/4 & 0 & 1/2 & 0 & 0 & 1/4 & 0 \\ 1/2 & 0 & 0 & 0 & 1/2 & 0 & 0 & 0 & 0 \\ 0 & 1/4 & 0 & 1/4 & 0 & 1/4 & 1/4 & 0 & 0 \\ 0 & 0 & 1/4 & 0 & 1/2 & 0 & 0 & 1/4 & 0 \\ 0 & 0 & 0 & 0 & 1/2 & 0 & 0 & 1/2 & 0 \\ 0 & 0 & 0 & 0 & 0 & 1/4 & 1/2 & 0 & 1/4 \\ 0 & 0 & 0 & 0 & 0 & 0 & 0 & 1 & 0 \end{pmatrix} \end{array} \tag{10}$$

Analytical values for update, U_{A_LU}, were calculated using equation 5. The process was then simulated and U_{S_LU} was calculated using equation 9.

Table 1 shows the analytical and simulated values obtained. It is assumed that the mobile user has made 20 steps (each step is a movement across a cell) including initial position. The relative error was computed in each case and is also tabulated in the third row.

Table 1: Average Location Update Rates – Square cell

Si	1	2	3	4	5	6
U_{A_LU}	4.6	4	3.8	3.4	3.2	3
U_{S_LU}	4.5949	3.9958	3.7908	3.4078	3.2016	2.9969
Rel error %	0.12	0.11	0.24	0.23	0.05	0.10

Si – Initial state of the user

From the table entries it can be seen that the relative error is less than 0.25% which indicates excellent concurrence between the analytically obtained values and the simulated values.

B. Location Update Rates - Hexagonal Cell Model

There are totally 15 computational states in the hexagonal model, out of which 11 are normal states and 4 are asterisk states for LA size n = 4. Table 2 tabulates the analytical and simulated values obtained using equations 5 and 9, after the mobile user has moved 20 steps (including initial position). The relative error is also tabulated and can be noticed to be less than 0.9%.

Table 2: Average Location Update rates – hexagonal cell

Si	1	2	3	4	5	6	7	8	9	10	11
Ua	3.8830	3.5333	3.3552	3.4563	2.8943	2.6132	2.6022	2.1630	2.0163	1.7210	1.5734
Us	3.8814	3.5352	3.3457	3.4510	2.8970	2.6180	2.59951	2.16241	2.0146	1.7366	1.5876
Rel error%	0.041	0.054	0.284	0.154	0.093	0.092	0.104	0.028	0.084	0.8981	0.894

Si – Initial state of the user

C. Dwell Time

For dwell time calculations, the regular transition matrix P given in section III is modified and reproduced below for an absorbing Markov chain. 'A' is the absorbing state.

$$P = [pij] = \begin{array}{c} \\ \mathbf{A} \\ \mathbf{1} \\ \mathbf{2} \\ \mathbf{3} \\ \mathbf{:} \end{array} \begin{array}{c} \begin{array}{ccccc} \mathbf{A} & \mathbf{1} & \mathbf{2} & \mathbf{3} & \mathbf{\ldots} \end{array} \\ \begin{pmatrix} p_{AA} & p_{A2} & p_{A3} & \ldots & \ldots \\ p_{1A} & p_{11} & p_{12} & p_{13} & \ldots \\ p_{2A} & p_{21} & p_{22} & p_{23} & \ldots \\ p_{3A} & p_{31} & p_{32} & p_{33} & \ldots \\ \ldots & \ldots & \ldots & \ldots & \ldots \end{pmatrix} \end{array} \tag{11}$$

C.1. Square Cell model

The transition matrix $\mathbf{P_a}$ for the absorbing Markov chain for the square cell model n=5 is given below:

$$\mathbf{P_a} = [\, p_{ij} \,] = \begin{array}{c} \\ A \\ 1 \\ 2 \\ 3 \\ 4 \\ 5 \\ 6 \end{array} \begin{array}{c} \begin{array}{ccccccc} A & 1 & 2 & 3 & 4 & 5 & 6 \end{array} \\ \begin{pmatrix} 1 & 0 & 0 & 0 & 0 & 0 & 0 \\ 1/2 & 1/2 & 0 & 0 & 0 & 0 & 0 \\ 1/2 & 1/4 & 0 & 1/4 & 1/4 & 0 & 0 \\ 1/4 & 0 & 1/2 & 0 & 0 & 1/4 & 0 \\ 0 & 0 & 1/2 & 0 & 0 & 1/2 & 0 \\ 0 & 0 & 0 & 1/4 & 1/2 & 0 & 1/4 \\ 0 & 0 & 0 & 0 & 0 & 1 & 0 \end{pmatrix} \end{array} \tag{12}$$

The dwell time was then estimated using simulation. The simulation process for dwell time is similar to the simulation process for location update. The average time to absorption is the sum of times to absorption divided by the number of experiments, M_E and is given as

$$\bar{M}(t) = \frac{1}{M_E} \sum_{x=1}^{M_E} M_i(t)(x) = U_{S\_D} \tag{13}$$

Table 3 shows the analytical and simulation values obtained for the dwell time for a 5 * 5 square cell configuration. The relative error was also calculated and was found to be less than 0.2%, which again validated the analytical approach.

Table 3: Average Dwell Time- square cell

S_i	1	2	3	4	5	6
$U_{A\ D}$	3.8077	5.6154	6.1538	8.5	9.3846	10.3846
$U_{S\ D}$	3.8011	5.6091	6.52543	8.5036	9.3905	10.3817
Rel error%	0.174	0.112	0.008	0.042	0.063	0.028

Si – initial state or cell of the mobile user

C.2. Hexagonal Cell Model

The validation for this part of analytical model was done with some published results as they were available. Hence instead of using the hexagonal model of size n=4, which we had used for studying the location update rates, we now use a hexagonal model of size n = 5 as published results were available for this configuration in [1]. Fig. 7 shows the numbering of cells and the transition probability matrix for hexagonal cell LA with n = 5. The asterisk boundary states of Fig. 5 have been lumped into an absorbing state to derive the dwell time. The 'A' in the transition matrix indicates the absorbing state. The analytical results obtained from our model are given in table 4. Also in the table we have given the simulated values from [1] for an identical configuration. The relative error tabulated is again within 0.4%. With this we have provided a second means of validation for the proposed mobility model.

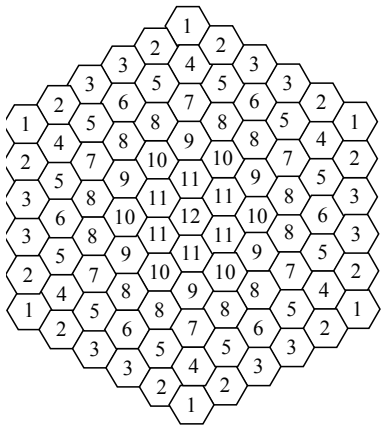

$P_a =$

	A	1	2	3	4	5	6	7	8	9	10	11	12
A	1	0	0	0	0	0	0	0	0	0	0	0	0
1	1/2	0	1/3	0	1/6	0	0	0	0	0	0	0	0
2	1/3	1/6	0	1/6	1/6	1/6	0	0	0	0	0	0	0
3	1/3	0	1/6	1/6	0	1/6	1/6	0	0	0	0	0	0
4	0	1/6	1/3	0	0	1/3	0	1/6	0	0	0	0	0
5	0	0	1/6	1/6	1/6	0	1/6	1/6	1/6	0	0	0	0
6	0	0	0	1/3	0	1/3	0	0	1/3	0	0	0	0
7	0	0	0	0	1/6	1/3	0	0	1/3	1/6	0	0	0
8	0	0	0	0	0	1/6	1/6	1/6	1/6	1/6	1/6	0	0
9	0	0	0	0	0	0	0	1/6	1/3	0	1/3	1/6	0
10	0	0	0	0	0	0	0	0	1/3	1/3	0	1/3	0
11	0	0	0	0	0	0	0	0	0	1/6	1/3	1/3	1/6
12	0	0	0	0	0	0	0	0	0	0	0	1	0

'A' **means absorbing state**

Fig. 5.6 Hexagonal cell LA and transition probability for absorbing Markov chain

Table 4: Dwell time - hexagonal cell (comparison with published results)

Si	1	2	3	4	5	6	7	8	9	10	11	12
Da	6.1423	8.5924	9.5516	13.6633	16.1979	16.9680	20.2578	22.2543	25.1793	26.1686	28.1722	29.1722
Ds	6.142	8.580	9.533	13.627	16.178	16.911	20.224	22.1	25.130	26.104	28.090	29.089
Rel error%	0.049	0.145	0.195	0.266	0.123	0.337	0.167	0.246	0.196	0.247	0.293	0.317

Si – Initial state of the user, Da – analytically obtained dwell time, Ds- dwell time from published results

V. Highlights of the Model

Before we apply the model to the overlapped location area strategy we highlight the features of the model that was described.

1. The number of computational states is considerably reduced. Some numerical examples on the state reduction is provided below. We have compared the number of states with a conventional model though work has been done by some researchers [1] to obtain reduced number of states.

A. Square cell:

For a normal square cell LA the computational states will $n \times n = n^2$ if a conventional 2-D random walk model were used. But in our model, the total states to be considered for computations are significantly reduced to

$$2 * \lceil n+1/2 \rceil^* + \sum_{n_i=1}^{n} \lceil n_i / 2 \rceil, \qquad (14)$$

where both n and n_i are odd

$$2^* \lceil n/2 \rceil^* + \sum_{n_i=2}^{n-1} n_i / 2, \quad (15)$$

where both n, n_i are even

In equations 14 and 15, the first part alone gives the boundary states, the second part gives the number of states that are not boundary states. Hence in the equations, the boundary states are multiplied by 2, to take into account the boundary asterisk states.

Taking a typical example, if n = 5, the number of computational states in the proposed model would be only 9 whereas in the conventional 2D model there would be 25 states.

B. Hexagonal cell:

The total number of states for conventional 2-D random walk model = $1 + \sum_{1}^{n} 6n$. The total number of states in the proposed model is given by

$$n^* + 1 + \sum_{1}^{n} n \, , \quad (16)$$

where n* are the number of asterisk states.

Taking a numerical example for n =4, the proposed model has 15 states, whereas the conventional model would have 61 states.

2. This regular Markov model so derived can be used for studying location update rates.
3. A slightly modified model with absorbing states, can be used to compute the LA dwell time.
4. The model can be applied for both square cells and hexagonal cells
5. The model can be used for static and dynamic location area strategies.
6. The calculation have been considerably simplified due to the wrap-around technique.

VI. Overlapped Location Area Modelling

To demonstrate the applicability of the proposed model to study an overlapped location area strategy, we have chosen the square cell configuration with size n = 5. In this study we will estimate the location update rates versus the inverse of 'Call to Mobility Ratio' (CMR), which we identify as the 'Movements Per Call' (MPC). This study was conducted for both - the non-overlapped and the overlapped cell configurations. Most location update studies, are conducted with respect to the CMR of the mobile user, hence we provide such a study here. Because of overlap, the LA boundary crossing rate decreases considerably as the size of the LA has expanded. However, since the total number of LAs is the same as when no overlapping is applied, the average number of mobile users per LA is the same for both overlapped and non-overlapped approaches.

Fig 7 shows a comparative picture of a normal LA with 25 square cells and an overlapped LA. Fig 7A shows the normal 25 cell LA with its adjacent LAs. If LA5 is the LA under consideration, then LA2, LA4, LA6 and LA8 are the adjacent LAs, to which the user can move from LA5. Fig. 7B shows the overlap between the adjacent LAs. The LAs are now called OLAs and the overlapped area of OLA5 is highlighted in Fig. 7B and is bounded by the bold broken lines. The corresponding overlap areas of the other LAs can be visualised – Overlap area of LA3 will be OLA3 as shown in Fig. 7C. The numbers in the cells correspond to the aggregate states identified within and LA earlier, though the numbering order has been changed for convenience of applicability in the overlapped case.

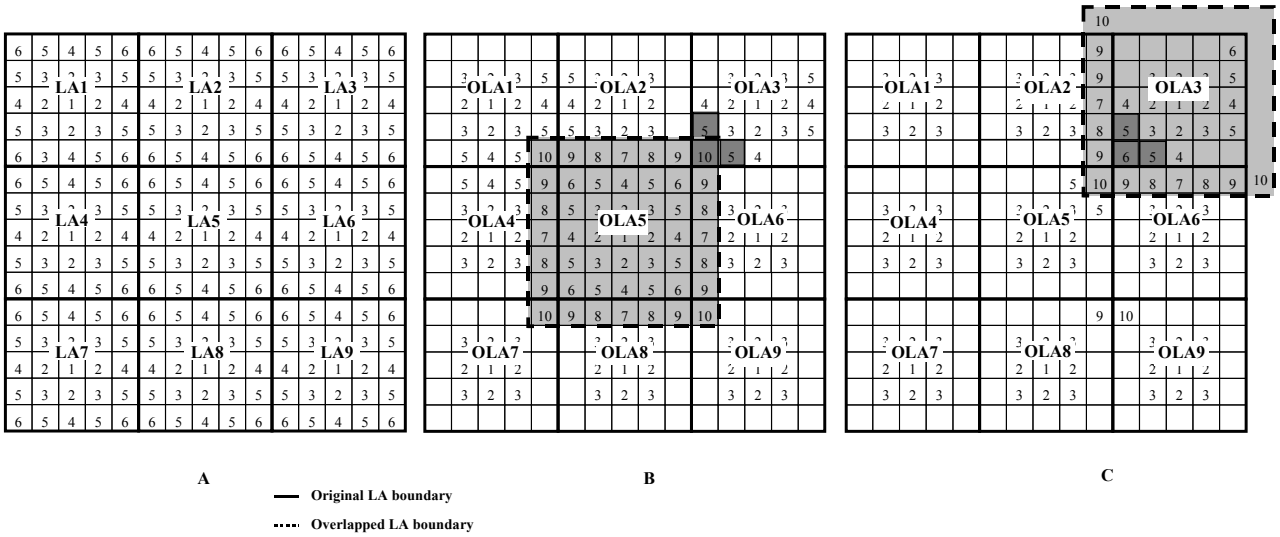

Fig. 7 Cell layout for overlapped LA

Fig. 7C has been provided to help explain the state transition diagram when the MT crosses from one overlapped LA to another, in this case from OLA5 to OLA3.

In the case of an overlapped LA such as OLA5, there are 10 aggregate states as can be seen in Fig. 7B. The state transition diagram for the MT movement within and across the boundary of the overlapped LA is given in Fig. 8. Fig. 8A shows the transitions within one overlapped LA and Fig. 8B shows the transitions from one overlapped LA to another.

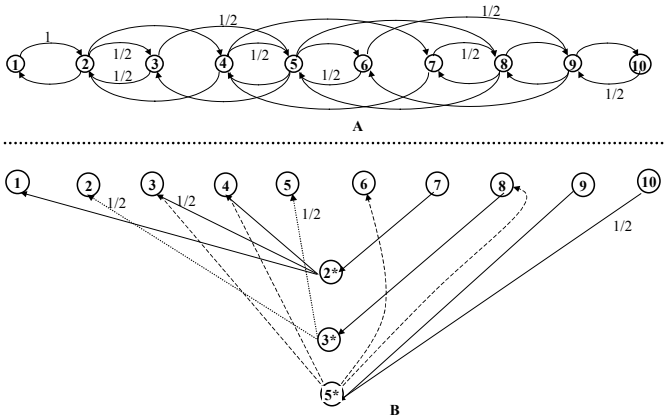

Fig. 8 State transition diagram for overlapped LA

Similar to the non-overlapped LA model, asterisk states 2^*, 3^*, and 5^* shown in Fig 8B represent the boundary states of adjacent OLAs.

A brief explanation of the state transition diagram is given here. Focusing on OLA5 and OLA3 in Figs. 7B and 7C, we explain the state transition diagram of Fig. 8. When a user is in state 10 in OLA5, he can transition to state 5 (dark shaded cells) in OLA3 with a ½ probability. (There are 2 adjacent state 5, and the transition to each is ¼). This is indicated as a transition from state 10 to state 5* in Fig. 8B with ½ probability. The mobile user can also move to state 9 (there are 2 state 9 adjacent to state 10) within LA5 itself with ½ a probability, which is shown in Fig. 8A. Once the user has left the overlapped area of OLA5, he is considered to be in the OLA3 coverage area. Hence if one refers to Fig 7C, the OLA3 extended area is explicitly shown. The dark shaded cells in Fig. 7C correspond to the dark shaded ones in Fig. 7B. We notice that the cell numbered 10 in the dark shaded cells of Fig. 7B is now a cell numbered 6 in OLA3 coverage area in Fig. 7C. From Fig. 7C the user in state 5 has a 1/4 probability of moving into state 3, 4, 6 or 8 which is indicated by the transition from 5* to state 3, 4, 6 and 8 in Fig. 8B. This explanation can be extended to understand how the transition diagram was derived. Once the state transition diagram has been obtained, the transition probability matrix can be obtained and this is given below.

$$P_{OLA} = [\, p_{ij} \,] = \begin{array}{c} \\ 2^* \\ 3^* \\ 5^* \\ 1 \\ 2 \\ 3 \\ 4 \\ 5 \\ 6 \\ 7 \\ 8 \\ 9 \\ 10 \end{array} \begin{array}{c} \begin{array}{cccccccccccccc} 2^* & 3^* & 5^* & 1 & 2 & 3 & 4 & 5 & 6 & 7 & 8 & 9 & 10 \end{array} \\ \begin{pmatrix} 0 & 0 & 0 & 1/4 & 0 & 1/2 & 1/4 & 0 & 0 & 0 & 0 & 0 & 0 \\ 0 & 0 & 0 & 0 & 1/2 & 0 & 0 & 1/2 & 0 & 0 & 0 & 0 & 0 \\ 0 & 0 & 0 & 0 & 0 & 1/4 & 1/4 & 0 & 1/4 & 0 & 1/4 & 0 & 0 \\ 0 & 0 & 0 & 0 & 1 & 0 & 0 & 0 & 0 & 0 & 0 & 0 & 0 \\ 0 & 0 & 0 & 1/4 & 0 & 1/2 & 1/4 & 0 & 0 & 0 & 0 & 0 & 0 \\ 0 & 0 & 0 & 0 & 1/2 & 0 & 0 & 1/2 & 0 & 0 & 0 & 0 & 0 \\ 0 & 0 & 0 & 0 & 1/4 & 0 & 0 & 1/2 & 0 & 1/4 & 0 & 0 & 0 \\ 0 & 0 & 0 & 0 & 0 & 1/4 & 1/4 & 0 & 1/4 & 0 & 1/4 & 0 & 0 \\ 0 & 0 & 0 & 0 & 0 & 0 & 1/2 & 0 & 0 & 0 & 0 & 1/2 & 0 \\ 1/4 & 0 & 0 & 0 & 0 & 0 & 1/4 & 0 & 0 & 0 & 1/2 & 0 & 0 \\ 0 & 1/4 & 0 & 0 & 0 & 0 & 0 & 1/4 & 0 & 1/4 & 0 & 1/4 & 0 \\ 0 & 0 & 1/4 & 0 & 0 & 0 & 0 & 0 & 1/4 & 0 & 1/4 & 0 & 1/4 \\ 0 & 0 & 1/2 & 0 & 0 & 0 & 0 & 0 & 0 & 0 & 0 & 1/2 & 0 \end{pmatrix} \end{array} \tag{17}$$

From Table 1, we get the average number of location updates made by a user making 20 steps. The entries in table 1 are tabulated against the starting cell position of the user – i.e. *Initial state* S_i. Assuming that there is an equal probability of finding the user mobile user in any one of the 25 cells, as his initial position, we can obtain the average number of location updates initiated by user moving within the LA and making k= 20 steps using the following equation

$$LU_n = \sum_{N=1}^{6} \text{Number of cells in aggregate state } S_N * U_{A\_LA} / (n \times n) \tag{18}$$

where LU_n is the average number of updates originating from a *normal* non-overlapped LA of size *n.*

The procedure was repeated for different values of *k.* If no call arrives between the *k* steps, then equation 18 gives the average number of updates made by a user roaming in the LA. Hence *k* gives the MPC values. We have evaluated the average number of location update rates for both the overlapped case and the non-overlapped case for various values of MPC and have provided them in Table 5.

Table 5. Location update versus MPC – overlapped and non-overlapped cases

MPC	1	2	3	4	5	6	7	8	9	10
overlapped	0.138	0.156	0.192	0.228	0.274	0.330	0.392	0.454	0.516	0.577
Non-overlapped	0.192	0.32	0.448	0.608	0.8	1.0	1.2	1.4	1.6	1.8

MPC	11	12	13	14	15	16	17	18	19	20
overlapped	0.639	0.701	0.763	0.825	0.887	0.949	1.010	1.134	1.134	1.196
Non-overlapped	2.0	2.2	2.4	2.6	2.8	3.0	3.2	3.4	3.6	3.8

The MPC carries similar information as CMR but is its inverse. The MPC shows the number of movements made by the mobile between two calls. For example, if we assume the average MPC is 20 then it means the mobile makes an average of 20 steps or movements across cells between 2 calls. We have used a range of specific values for MPC for obtaining the average number of location updates initiated by a user roaming within an LA. The entries in the table clearly show that the overlapped LA mechanism has less LA update requirements than the normal LA, which is true. Figure 5 is plot of the location updates calculated for the normal LA case and the overlapped LA case. From the graph we notice that the more number of movements a user makes between call arrival, which signifies that he is a fast moving user, the average number of updates increases with increasing MPC. However for the overlapped LA case the number of location updates is considerably less, especially at higher MPC values, which is logically reasonable.

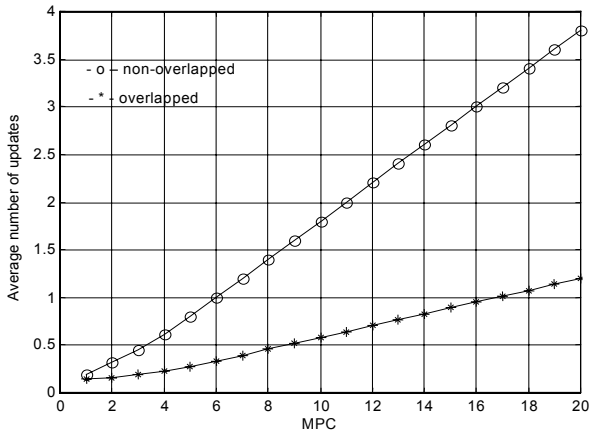

Fig.9 LA updates and overlapped LA updates versus MPC

VI Conclusion

Applying 2D random walk models to study user mobility in terms of location updates and dwell time in wireless networks has been difficult due to the number of computational states, which one encounters in analytical models. In this work we applied the property of 'lumped process' to the regular Markov chain and obtained a model with reduced computational states. The model could be used to study location update rates and dwell time both for the square cell and hexagonal cell configurations. The analytical results obtained for location update and dwell time for the two configurations,(square and hexagonal) show excellent agreement with the simulation results with relative error less than 1%. The model was further validated with published results. The adaptability of the model has been demonstrated by applying it to an overlapped square cell LA case.

Reference:

[1] I. F. Akyildiz, Y.-B. Lin, W.-R. Lai, R.-J. Chen, "A new random walk model for PCS networks," *IEEE Journal on Selected Area in Communication*, vol. 18, no. 7, July 2000, pp. 1254-1259.
[2] K. S. Meier-Hellstern, E. Alonso, "The use of SS7 and GSM to support high density personal communications," *Proceedings of IEEE ICC'92*, Chicago, IL, June 1992, pp. 1698-1072.
[3] S. Mohan, R. Jain, "Two user location strategies for personal communications services," *IEEE Personal Communications*, vol.1, no. 1, 1st Qtr. 1994, pp. 42-50.
[4] G. P. Pollini, D. J. Goodman, "Signalling system performance evaluation for personal communications," *IEEE Transactions on Vehicular technology*, vol. 45, no. 1, Feb. 1996, pp. 131-138.
[5] B. Jabbari, Y. Zhou, F. Hellier, "Random walk modelling of mobility in wireless networks," *Proceedings of IEEE VTC'98*, May 1998, pp. 639-643.
[6] T. X. Brown, S. Mohan, "Mobility management for personal communications systems," IEEE *Transactions on Vehicular technology*, vol. 46, no. 2, May 1997, pp. 269-278.
[7] I. F. Akyildiz, J. S.M. Ho, Y.-B. Lin, "Movement-based location update and selective paging for PCS networks," *IEEE/ACM transactions on Networking*, vol. 4, no. 4, Aug. 1996, pp. 629-638.
[8] D. Lam, D. C. Cox, J. Widom, "Teletraffic modelling for personal communications systems," *IEEE Communications Magazine*, vol. 35, no. 2, Feb. 1997, pp. 79-87.
[9] K.-H. Chiang, N. Shenoy, "Architecture and schemes for intelligent mobility management in future mobile telecommunication systems," *Proceedings of IEEE GLOBECOM'00*, San Francisco, CA, Nov. 2000, pp. 1463-1467.
[10] J. G. Kemeny, J. L. Snell, *Finite Markov Chains*. New York: Springer-Verlag, 1976.
[11] Tuna Tugcu, Cem Ersoy, "Application of Realistic mobility model in metropolitan cellular systems", Vehicular Technology Conference VTC 2001, Spring, Rhodes, Greece, May 2001.
[12] Su W., Lee S. -J., Gerla M., "Mobility prediction in Wireless Networks", Proceedings of IEEE MILCOM 2000, Los Angeles, CA Oct 2000.
[13] Markoulidakis J. G., Lyberopoulos G. L., Tsirkas D.F. and Sykas E. D., " Mobility Modelling in Third Generation Mobile Telecommunications Systems", IEEE Personal Communications pp 41-56, August 1997.
[14] Leung K. K., Massey W. A.,and Whitt W., "Traffic Models for Wireless Communications Networks", IEEE Journal of Selected Areas in Communications, Vol 12, No. 8, pp 1353-1364, Oct 2000.
[15] Kuo-Hsing Chiang, Nirmala Shenoy, "A Random Walk Mobility Model for Location Management in Wireless Networks", PIMRC 2001, San Diego
[16]M Mouly, M. B. Pautet, *The GSM system for mobile communications*. Published by authors, 1992.
[17] EIA/TIA, "Cellular radio-telecommunications intersystem operations," *Technical Report IS-41*, Revision C, 1995.